


 Cite this: *Lab Chip*, 2024, 24, 4085

## ElectrochemCap: an integrated detection for loop-mediated isothermal amplification reactions†

 P. Rioboó-Legaspi,  E. Costa-Rama \* and M. T. Fernández-Abedul \*

Loop-mediated isothermal amplification (LAMP) of genetic materials has emerged as a powerful molecular biology technique with great potential to be a standard point-of-care (POC) technique. This method has found several applications, but it still presents challenges for its direct on-site application, particularly in terms of integrated reaction and detection systems and the risk of carryover contamination. In this work, we propose an innovative solution – an electrochemical microcentrifuge tube cap (ElectrochemCap) based on a screen-printed electrode, a 3D printed adapter and an adhesive layer – which integrates the amplification reaction and its subsequent electrochemical detection in a single device. The design, fabrication, and electrochemical characterization of the ElectrochemCap are reported here, demonstrating its suitability for LAMP detection. Rapidly emerging technologies, such as 3D printing or xurography, are the basis of a prototype that has been validated for the detection of SARS-CoV-2 using reverse transcription LAMP (RT-LAMP), achieving results comparable to those obtained by gold-standard RT-qPCR. Moreover, we have explored the versatility of the ElectrochemCap presenting several additional designs (for containers with different volumes, shapes and materials, as well as multiplexed approaches), expanding its potential applications. Overall, the ElectrochemCap represents an affordable, versatile, and marketable innovation for integrated quantitative electrochemical detection, with enormous possibilities in bioelectroanalytical procedures and portable laboratory setups.

 Received 5th May 2024,  
 Accepted 5th July 2024

DOI: 10.1039/d4lc00395k

[rsc.li/loc](https://rsc.li/loc)

### Tribute to George Whitesides

I wanted to know George and the science behind his well-written papers, with their introductions, purposes, and results obtained from simple but creative devices. Happily, I got the answer: “Summers are busy with visitors. I would like to make sure that the stay would be useful for you and possibly for us”. I cannot explain all I learned, but here are a few lessons: i) speak (and publish) only when you have something important to say; ii) involve people in research and make them want to collaborate; iii) be interdisciplinary; iv) aim for excellence and welcome corrections: “If the reviewer is asking, it is because we haven’t explained it well”; v) be humble: “Now that you see the group from the inside, what do you think we should improve?”; vi) take care of people, they matter; help those deserving and give credit where it is due; avoid excessive self-referencing; vii) be strict, starting with yourself; viii) fun is the important motivation.

Many view science as something ahead, like a soap bubble, difficult to catch. However, I see George as “the man inside the bubble”. He moves science from there and, occasionally, small bubbles, full of knowledge, come out to the delight of followers. We were lucky to put our heads in the bubble for a while and look from the inside. Thanks once again for these wonderful summers, the memories, and the opportunity to meet you (and Barbara) and work with skilled researchers, as well as with TJ and Melissa. I was right, I had to go, and fortunately, I went. Happy 85th birthday, George! – *M. Teresa Fernández Abedul*

## Introduction

Loop-mediated isothermal amplification or LAMP has become a key molecular biology technique in the recent years. This technique, first described in 2000,<sup>1</sup> is performed

at *ca.* 65 °C and relies on the use of 4 or 6 primers and a polymerase with strand-displacement activity for the formation of loop-shaped secondary structures, resulting in dumbbell-like amplicons. This produces a highly efficient amplification, leading to fast results even with a low copy number of the template,<sup>2</sup> all of this without requiring temperature cycling.

LAMP reactions have been widely used in the field of diagnostics, *e.g.*, infectious diseases (viral, fungal, or bacterial), study of gene expression, mutation detection or transcript

Departamento de Química Física y Analítica, Facultad de Química, Universidad de Oviedo, Spain. E-mail: [costaestefania@uniovi.es](mailto:costaestefania@uniovi.es), [mtfernandeza@uniovi.es](mailto:mtfernandeza@uniovi.es)

† Electronic supplementary information (ESI) available. See DOI: <https://doi.org/10.1039/d4lc00395k>



analysis, among others.<sup>3</sup> Other fields where this technique has become a keystone are food quality control, for detection of pathogens<sup>4</sup> and toxins,<sup>5</sup> and others such as animal health,<sup>6</sup> forensics<sup>7</sup> or biosecurity.<sup>8</sup> Regarding detection, optical techniques, with mainly colorimetric (visual)<sup>9</sup> or fluorimetric<sup>10</sup> readout, have been widely used. However, when naked-eye detection is employed, the sensitivity and limit of detection cannot be compared to those obtained by using instrumental methodologies. The use of equipment for reliable quantitative optical measurements is still hard to implement for rapid and low-cost approaches.<sup>11</sup> Electrochemical techniques provide cheap and simple detection setups, providing sensitive and robust quantitative information.<sup>12</sup>

This isothermal amplification with electrochemical detection (LAMP-ED), however, still presents a few limitations for its direct application to on-site diagnosis. The first one is the need of an integrated device, so that the amplification reaction and the electrochemical detection can be easily performed in a single step. The second one is the presence of carryover contamination. LAMP reactions produce a very high number of amplicons, and thus the manipulation of the products of the reaction can easily contaminate materials and reagents employed in further amplifications, reading all the reactions as positive, independent of their initial copy number.<sup>13</sup>

Both problems can be easily solved by integrating both steps, reaction and detection, into a single all-in-one device. Thus, once the sample and the initial reaction mix are added to the reaction container, no further manipulation is required. So far, most of the electrochemical LAMP-based approaches perform the reaction in a microcentrifuge tube. Later, the content is transferred to a screen-printed electrochemical (SPE) cell where the electrochemical measurement is performed.<sup>14–17</sup> Some integrated devices have been proposed in the literature, in many cases relying on microfluidics to create a reaction chamber where LAMP can take place.<sup>18,19</sup> However, these examples, albeit interesting, are either complex and expensive in their manufacturing or have not achieved a full degree of integration. Other interesting approaches combining both steps still rely on centralized equipment<sup>20</sup> or are based on custom-made electrochemical cells.<sup>21</sup>

An easy, affordable solution is the development of an integrated device where the cap of a microcentrifuge tube would act as the electrochemical cell of the device. In this sense, the reaction would take place far from the electrode, in an airtight environment. Once completed, the reaction solution would contact the electrode surface by simply flipping the device. This kind of device would offer: i) the integration of reaction and detection, with no transfer steps needed; ii) an airtight reaction chamber, with little to no volume loss; iii) the prevention of LAMP carryover contamination, as no manipulation of the products is required, and, iv) the availability of a simple tool that, combined with portable potentiostats,<sup>22</sup> can be easily used at the point-of-care.

So far, research on cap-based integrated electrochemical devices is still under development, with only a few examples reported. Initial approaches of cap-based devices integrated SPEs on caps of larger containers, such as screwcap glass vials, for direct determination of heavy metals in water.<sup>23</sup> Further approaches have been tuned towards other current laboratory materials, such as microcentrifuge tubes, where simpler and cheaper electrochemical cells were included. The use of already mass-produced elements, such as metallic pins,<sup>24</sup> as electrodes was proposed for the determination of stroke biomarkers.<sup>25</sup> Regarding LAMP procedures, few approaches have been described. A LAMP-based electrochemical sensor for genetically modified organisms (GMOs) was based on a device where the reaction tube was connected to a SPE *via* a detection cap.<sup>26</sup> Here, the amplification product was mixed with the redox probe Hoechst 33258 after breaking a valve and inverting the tube. This would prevent the inhibition of the LAMP reaction by the redox probe. More recently, an E-Tube, where the cap acted as both a system for DNA extraction from the sample, with a purification membrane incorporated, and a pH electrode to measure the pH drop caused by the LAMP reaction, was developed.<sup>27</sup>

However, these approaches are complex either in fabrication or handling, or are made for a very specific goal, thus hampering its widespread use. To fill this gap, we propose a very simple, intuitive, and innovative approach based on the incorporation of a flat and flexible commercial SPE into a homemade 3D-printed microcentrifuge tube cap, creating a device suitable for LAMP detection, but also for several other (bio)electroanalytical applications. The device is fabricated using 3D printing and xurography, techniques that have arisen as powerful tools for simple, fast and scalable fabrication of different electroanalytical devices.<sup>28</sup> 3D printing, in particular, fused deposition modelling, has been widely used for the fabrication of electrochemical biosensors. The popularity of this technique relies on rather inexpensive equipment, very little to no post-processing steps and a wide variety of commercially available filaments, such as flexible, soluble or conductive filaments.<sup>29</sup>

This electrochemical SPE-based microcentrifuge tube cap (ElectrochemCap) could be very appropriate for real implementation of low-cost diagnostics. This device has been electrochemically characterized both for general purposes and for direct LAMP applications, with outstanding results.

## Materials and methods

### Reagents

Potassium ferrocyanide, PBS tablets, methylene blue, Trizma base, EDTA, boric acid, phosphoric acid and acetic acid were purchased from Sigma-Aldrich. All chemicals employed were of analytical reagent grade. Water was purified using a Direct-Q® 3 UV Milli-Q system (Merck).



## RT-LAMP assay

The RT-LAMP methodology used was based on a previous work,<sup>30</sup> adapting the procedure to a final volume of 50  $\mu\text{L}$ . The method and primers used can be found in the ESI† (procedure 1 and Table S1). All reactions were performed in 0.2 mL low-retention microcentrifuge tubes provided with the ElectrochemCap for further quantitative detection.

## Design and fabrication of the ElectrochemCap

The ElectrochemCap is composed of a 3D-printed thermoplastic polyurethane (TPU) casing adhered to a commercial screen-printed electrochemical cell (SPE) using a pressure-sensitive adhesive (PSA, Adhesives Research®). The 3D casing was printed with clear TPU (Geetech) using a Creator 3 Pro 3D printer (FlashForge). The 3D-printed casing was designed with Autodesk Tinkercad and sliced with the software Flash Print 5 (FlashForge). The adapter was printed with a layer height of 0.18 mm, a 15% hexagon infill, a printing speed of 60 mm s<sup>-1</sup> (no retraction), and extruder and bed temperatures of 230 and 55 °C, respectively. The PSA layer was fabricated by xurography<sup>31</sup> using Silhouette Studio software for designing the PSA layers and cut with a cutter plotter (Silhouette Portrait 2, Silhouette America). The containers used for the device were 0.2 mL low-retention, nuclease-free PCR grade microcentrifuge tubes (PCR-02-L-C, Axygen™), 1.5 mL microcentrifuge tubes (PCRD-015-500, astiKs), flat-bottomed 1.5 mL polymeric tubes (astiKs) and 2 mL screwcap glass vials (SVP2-A02-100, Metria).

## Electrochemical detection (ED)

Electrochemical measurements of the amplifications were performed connecting the ElectrochemCap to a  $\mu\text{AUTOLAB}$  TYPE III potentiostat (Metrohm), which was controlled with NOVA Software 2.1.5 (Metrohm), through a box connector (ED-SPE-BOX, MicruX Technologies). The SPEs used (S1PE, MicruX Technologies) were three-electrode screen-printed cards (27.5 × 10.1 × 0.35 mm, 350  $\mu\text{m}$  thick PET white substrate) consisting of a 3 mm diameter circle-shaped (with an area of 7.1 mm<sup>2</sup>) working electrode (WE) and a hook-shaped counter electrode (CE), both made of carbon ink, and a reference electrode (RE) made of silver ink. A design for cells containing two carbon working electrodes (D2PE, MicruX Technologies) was also proposed. In this case, the card consisted of two parallel carbon slots (1.0 × 2.5 mm, *i.e.*, an area of 2.3 mm<sup>2</sup>) acting as working electrodes, and a hook-shaped carbon counter electrode that surrounds both the 2 WEs and the reference electrode, a silver-ink slot perpendicular to both WEs. To perform the electrochemical measurements, the microcentrifuge tube closed with the corresponding ElectrochemCap was inverted, depositing the whole volume of the reaction over the electrodes of the SPE cell. Measurements were performed at room temperature and one electrochemical card, *i.e.*, one ElectrochemCap, was used for each measurement.

## Sample collection

Nasopharyngeal (NP) samples were collected using flocked nylon swabs (SW01E, Biocomma Ltd.) at the Central University Hospital of Asturias (HUCA). NP swabs were deposited into tubes containing 500  $\mu\text{L}$  of 10 mM Tris-EDTA buffer (TE, pH 8.0). The samples were inactivated by heat (95 °C for 5 min) prior to their transportation outside hospital facilities.<sup>32</sup> This study was carried out in accordance with the recommendations of the Ethical Committee on Regional Clinical Research of the Principality of Asturias (ref. 2024.016).

## Statistics

Results in this study are represented as mean value  $\pm$  standard deviation (SD). Relative standard deviations (RSDs) are calculated as the ratio between the SD value and its corresponding mean, in percentage.

## Results and discussion

### Design and electrochemical characterization of the device

To create an integrated device where a screen-printed electrode-based card could serve as both the cap of the microcentrifuge tube and the electrochemical cell for the detection of a LAMP reaction, a flexible plastic piece is needed as an interface. Thus, the tube containing the master mix and the card would snap in place creating an airtight sealing. When required, the tube would be inverted and then the electrochemical cell could be used for detection since the contents of the tube can flow down to the screen-printed card without leaking. Therefore, an all-in-one platform is obtained, where reaction and detection can occur sequentially.

In general, the ElectrochemCap consisted of a simple, flexible TPU piece with a cavity attached to the SPE electrochemical cell *via* a PSA layer (Fig. 1A, left). In the initial prototype (model 1 in Fig. 1A, right), a cylindrical cavity was designed (volume of  $\sim 150 \mu\text{L}$ ). To evaluate the electrochemical behaviour, 50  $\mu\text{L}$  of 5 mM potassium ferrocyanide solution in PBS was deposited on the tube, fitting the ElectrochemCap. If a reaction occurs, the position of the tube is kept upwards until detection. In this case, as there is no reaction, the device was turned upside down, as shown in the schematics in Fig. 1B (left), for electrochemical measurement. In the cyclic voltammogram recorded (Fig. 1B, right), the oxidation of ferrocyanide and the corresponding reduction of ferricyanide were observed. However, this was an irreversible process with an unusually high oxidation potential as well as a very diminished reduction current. When performing these measurements, it was observed that the tube was in contact with the reference and counter electrodes.

To overcome this limitation, a second prototype (model 2 in Fig. 1A, right) was designed. This model, aside from the initial cylindrical cavity, presented a lower conical feature to create an overhang that would prevent the tube from touching the SPE. In this case, there would be a conical chamber between the SPE and the edge of the tube. When



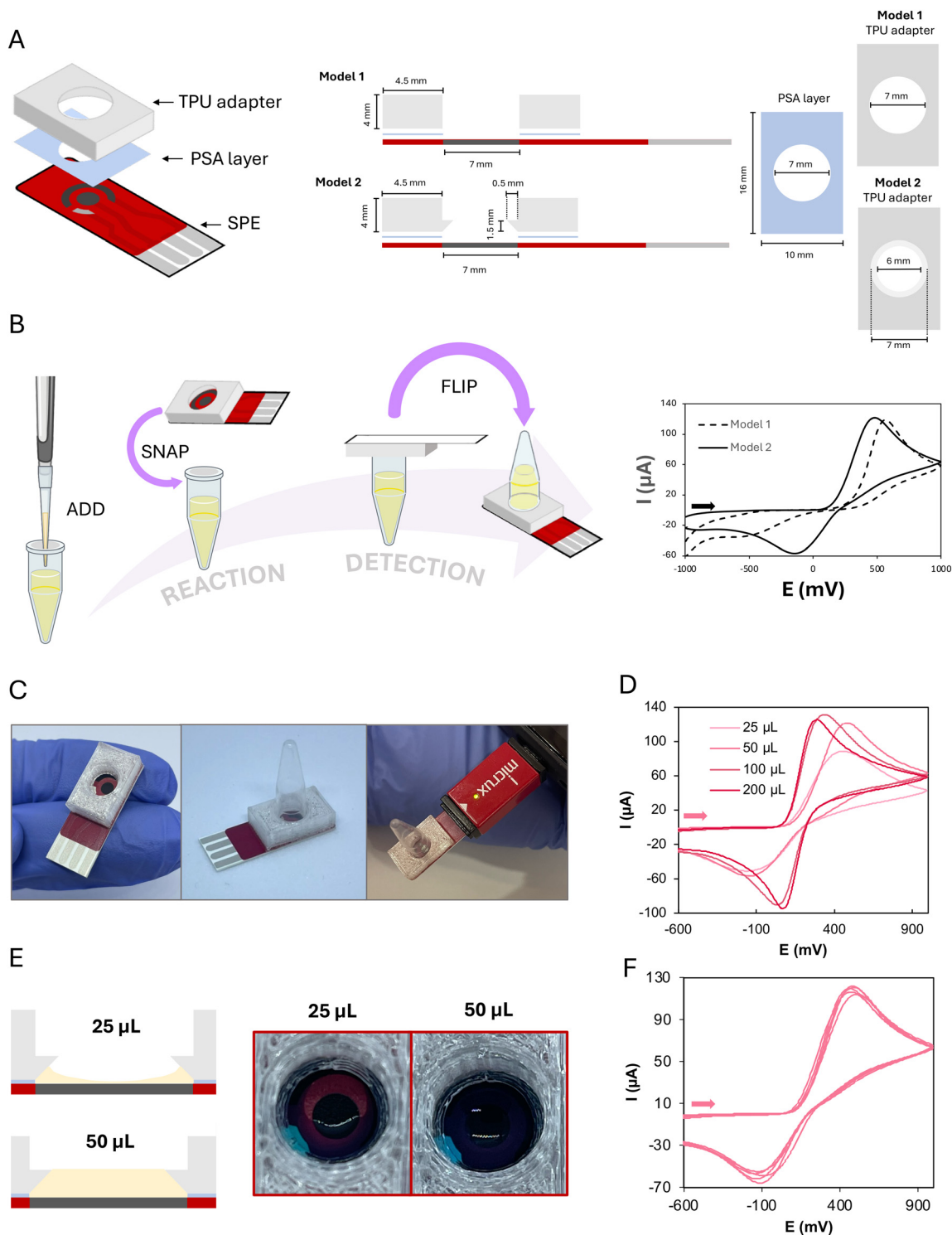


**Fig. 1** Design and characterization of the ElectrochemCap. **A**) Specifications of the two models designed. Left: General overview of the ElectrochemCap. Right: Dimensions and layout of the fabricated pieces, models 1 and 2. **B**) Left: Schematics of the procedure for a general electrochemical determination using the ElectrochemCap. Right: CVs recorded with model 1 and model 2 in 50  $\mu\text{L}$  of 5 mM  $\text{K}_4[\text{Fe}(\text{CN})_6]$  in PBS (pH 7.2). **C**) Pictures of the ElectrochemCap showing only the cap itself (left) and the flipped full device including the microcentrifuge tube (center), connected to a portable potentiostat (right). **D**) CVs recorded using different volumes of 5 mM  $\text{K}_4[\text{Fe}(\text{CN})_6]$  in PBS (pH 7.2). **E**) Schematic representation (left) and pictures depositing in the cap 25 and 50  $\mu\text{L}$  of 0.01% methylene blue solution in water (right). **F**) Successive CVs ( $n = 5$ ) of 50  $\mu\text{L}$  of 5 mM  $\text{K}_4[\text{Fe}(\text{CN})_6]$  in PBS (pH 7.2) recorded with the ElectrochemCap. The scan rate for recording CVs was  $0.1 \text{ V s}^{-1}$ .



inverting the tube, this conical part would be filled up with the solution, covering all the three SPEs. The electrochemical behaviour obtained for this model is shown in Fig. 1B (right), more convenient than this observed for model 1. Thus, this model, now named ElectrochemCap (Fig. 1C) was the one chosen to carry out this work.

The possible influence of the volume added to the tube on the electrochemical behaviour was evaluated. This is a crucial parameter, as this tube was initially designed for LAMP reactions, where the volume usually spans from 25 to 50  $\mu\text{L}$ . As it can be observed in Fig. 1D, the performance of the ElectrochemCap heavily depends on the measurement volumes, where 200 and 100  $\mu\text{L}$  of 5 mM potassium ferrocyanide solution present a quasi-reversible process ( $\Delta E_p = 215$  mV with  $I_{pa}/I_{pc} = 1.04$  for 200  $\mu\text{L}$ ). The oxidation current for 50  $\mu\text{L}$  approaches those for 100 and 200  $\mu\text{L}$  although the electron transfer is not as fast, as demonstrated by the difference in peak potentials and the ratio between anodic and cathodic peak currents. When 25  $\mu\text{L}$  is deposited, a CV with a lower anodic current intensity is shown. This volume seems not to be enough for the full coverage of the electrodes of the SPE, as it tends to form a meniscus-like shape with the TPU piece (Fig. 1E). This is not so notorious in the case of 50  $\mu\text{L}$ , where the volume of the truncated cone ( $\sim 50$   $\mu\text{L}$ ) could be filled with the sample solution and the weight of the solution is higher, pushing the solution to the electrode surface. Although 100 and 200  $\mu\text{L}$  show a more appropriate electrochemical behaviour, 50  $\mu\text{L}$  was used for the rest of the studies as required for the LAMP reactions, as a compromise between electrochemical performance and scale-up associated costs.

When evaluating the precision based on the volume used, it can be clearly noted that 25  $\mu\text{L}$  presents relative standard deviations (RSDs) of 7% for  $E_{pa}$  and 55% for  $I_{pa}$  (Fig. S1A<sup>†</sup>), while 50  $\mu\text{L}$  presents the best combined results, with RSDs as low as 3% for both  $E_{pa}$  and  $I_{pa}$  ( $n = 5$ , Fig. 1F). The excellent precision in the potential for 50  $\mu\text{L}$  is very important, since the analytical signal employed for the quantitative analysis of LAMP reactions is a peak potential. Signals corresponding to volumes of 100 and 200  $\mu\text{L}$  also present adequate precision (RSDs  $\leq 4\%$ ,  $n = 5$ , Fig. S1B and C<sup>†</sup>).

The integration of both steps in the same, now multifunctional, container has several advantages over off-line approaches: i) it largely simplifies the procedure, shifting from liquid transfer steps that would need additional materials (e.g., micropipettes, tips...) to easier operations. This is important not only for reducing the time and the cost of consumables but also to increase the precision of the methodology by avoiding human operation. ii) Apart from this, by using the same container, biological contamination is avoided. Since LAMP is a very sensitive technique and many copies are produced, this becomes of paramount relevance. With the ElectrochemCap, opening the tube for detection is not required and amplicons remain confined inside. iii) Different parts of the container for different

operations are used. Thus, the material and volume of the microcentrifuge tube are appropriate for LAMP reactions, without interference from those materials required for detection (conductive carbon and silver inks for electrodes and dielectric materials for isolating the connections and delimiting the cell) or those for adapting the tube to the cap (either TPU or PSA). On the other hand, the reaction medium can contain reagents that could be adsorbed on the electrode surface decreasing the effective electroactive area. With this cap, the surface of the electrode is maintained clean for further detection, with no interaction between materials and reaction solution. The storage stability of the components, regarding e.g., possible oxidative or UV-degradation processes of TPU,<sup>33</sup> should be evaluated in case the device is going to be stored for a long time. iv) The equipment and conditions required for each operation (reaction or detection) are compatible with one another. In this case, applying 65  $^{\circ}\text{C}$  for 30 min is required in LAMP reactions. Since an isothermal procedure is performed, it does not require thermocycling and heat can be provided with a laboratory heater or oven. On the other hand, the electrochemical cap provides a tight sealing after placing the integrated platform on the tube. Regarding the equipment needed for electrochemical measurements, a potentiostat can be easily connected, either directly or through an interface, depending on the type of potentiostat is employed (portable or benchtop, respectively).

The economic cost of the device itself, aside from the instrumentation required for its fabrication, is  $\sim 1.60$  EUR/1.80 USD. The individual costs are shown in Table S2,<sup>†</sup> where the price itself is only  $\sim 0.10$  EUR or USD over the cost of the SPE cell. This converts it into a very affordable and marketable innovation, opening the door for less expensive approaches if self-produced electrodes are used. It can also be noted that the most expensive component, when integrating a biological reaction such as LAMP, is the cost of the reaction itself, as can be also seen in Table S2.<sup>†</sup> Reduction of the volume would alleviate costs.

### ElectrochemCap for LAMP reactions: application to SARS-CoV-2 detection

Based on the previous results, the use of the device was evaluated for LAMP reactions. The determination used here is based on the pH-dependent electrochemical behavior of phenol red (PR), a common visual indicator of LAMP reactions.<sup>34</sup> This molecule is already included in the master mix and changes from red to yellow as the pH drops ( $\text{p}K_a = 7.9$ , 0.1 M Britton–Robinson buffer solution). This electroactive indicator presents an irreversible process, anodic, with a peak potential that shifts with pH. As amplification progresses, protons are liberated, and a pH drop is expected. Thus, the difference between final and initial potentials ( $\Delta E_p$ ) is an adequate analytical signal that can be correlated with the initial number of nucleic acid copies, as it has been already demonstrated for the pneumolysin gene of *Streptococcus pneumoniae*<sup>34</sup> and the N1 fragment of SARS-CoV-



2.<sup>30</sup> To evaluate the signal obtained with the fully integrated device, the peak potential ( $E_p$ ) for the oxidation of PR, obtained for different pH values, was represented against pH (Fig. 2A). The characteristic peak shift, with lower pH values showing higher  $E_p$ , can be observed. The device responds as expected in the pH range of LAMP reactions using this colorimetric, also electroactive, indicator. Furthermore, as the analytical signal is the shift of the oxidation peak potential, linear sweep voltammetry (LSV) could be employed instead of CV (inset of Fig. 2A). The use of this electrochemical technique results in faster analyses. In this way, after including the master mix and

sample, the reaction and detection would take place in the same container, with the indicator (PR) already included in the master mix and the detection element in the cap. Thus, minimal intervention, without any additional step, is required. Furthermore, the PR oxidation process recorded in more acidic and alkaline conditions is presented in Fig. S2,<sup>†</sup> opening the door for the use of this platform under conditions other than those presented here.

With the ElectrochemCap tested for pH-based PR oxidation peak shift, the device was used for LAMP amplification quantification. For this purpose, a set of RT-LAMP reactions

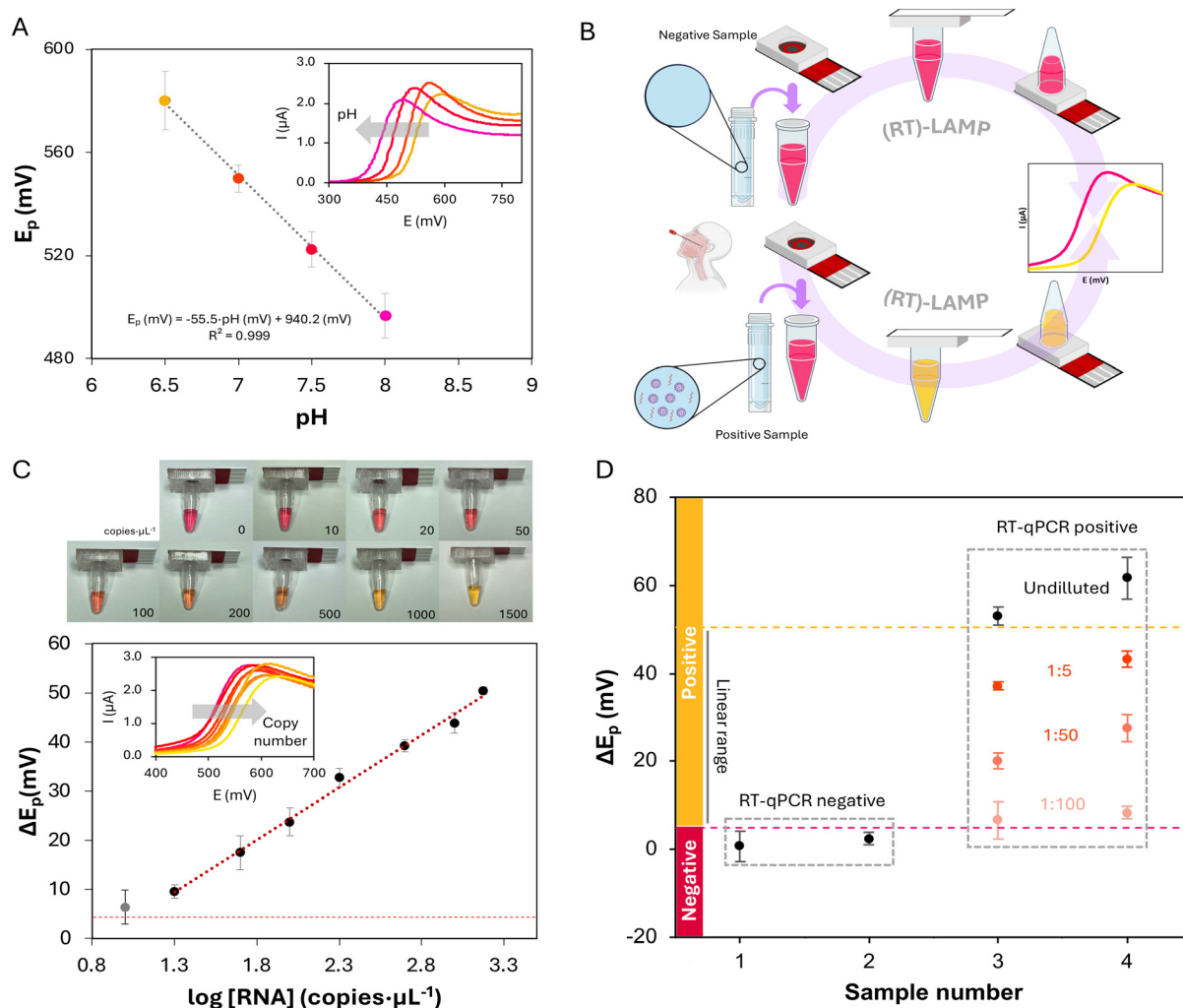


**Fig. 2** ElectrochemCap for LAMP application. A)  $E_p$  recorded by LSV for PR at different pH values, measured with the ElectrochemCap. Inset: LSVs recorded with the ElectrochemCap in 100  $\mu\text{M}$  PR in 10 mM PBS solutions of different pH (left to right, pH 8.0 to 6.5). B) Procedure for SARS-CoV-2 detection performing RT-LAMP in 0.2 mL tubes with the ElectrochemCap. C) Top: Pictures of the tubes with the ElectrochemCap used for RT-LAMP-ED, after the amplification. Copies per  $\mu\text{L}$  are indicated below each picture. Bottom: Calibration curve for SARS-CoV-2 standards obtained by RT-LAMP performed with the ElectrochemCap. The horizontal red dashed line indicates 3 times the standard deviation of the blank (0 copies per  $\mu\text{L}$ ). The grey dataset represents the value for 10 copies per  $\mu\text{L}$ . Inset: LSV curves for each initial copy number (left to right, 10, 20, 50, 100, 200, 500, 1000 and 1500 copies per  $\mu\text{L}$ ). D) Sample analysis using the ElectrochemCap for RT-LAMP-ED. NP samples are classified under a sample number (1 to 4), and their respective RT-qPCR result (positive or negative) is indicated by a grey dashed box. The dashed red line indicates the cutoff level, distinguishing between negative and positive samples. The dashed yellow line indicates 3 times the standard deviation of the upper limit of the linear range (below the limit) obtained with the methodology proposed here. Dilutions of samples 3 and 4 are shown below their undiluted results (black set) indicating the dilution performed. Error bars in all the cases represent the standard deviation for 3 replicates. The scan rate for LSV was  $0.1 \text{ V s}^{-1}$ .



were performed using SARS-CoV-2 LAMP primers for a segment of the N gene and SARS-CoV-2 RNA standard. The procedure is shown in Fig. 2B for negative and positive samples. The sample (or standard) solution would be added into a PCR microcentrifuge tube containing the LAMP reaction mix (including the reaction buffer, nucleotides, *bst* polymerase, primers and PR). The tube is then closed using the ElectrochemCap and the reaction is performed in a heater at 65 °C. After 30 min, the reaction is completed and can be first observed visually. It is important to note that as the device is fully closed and does not have to be opened after the reaction

takes place, addition of uracyl-DNA glycosylase (UDG) is not needed. The use of this enzyme is, however, crucial in those assays where the reaction products are manipulated as it can lead to carryover contamination.<sup>29,31</sup> For an electrochemical quantification, the tube is inverted so that the content flows towards the ElectrochemCap and, after connecting the device to a potentiostat, an LSV curve is recorded, measuring the anodic peak potential of PR. As the LAMP reaction progresses, protons and pyrophosphate anions are released, decreasing the pH of the reaction. Reactions with a higher initial copy number would lead to a higher pH drop and thus a bigger shift in the oxidation

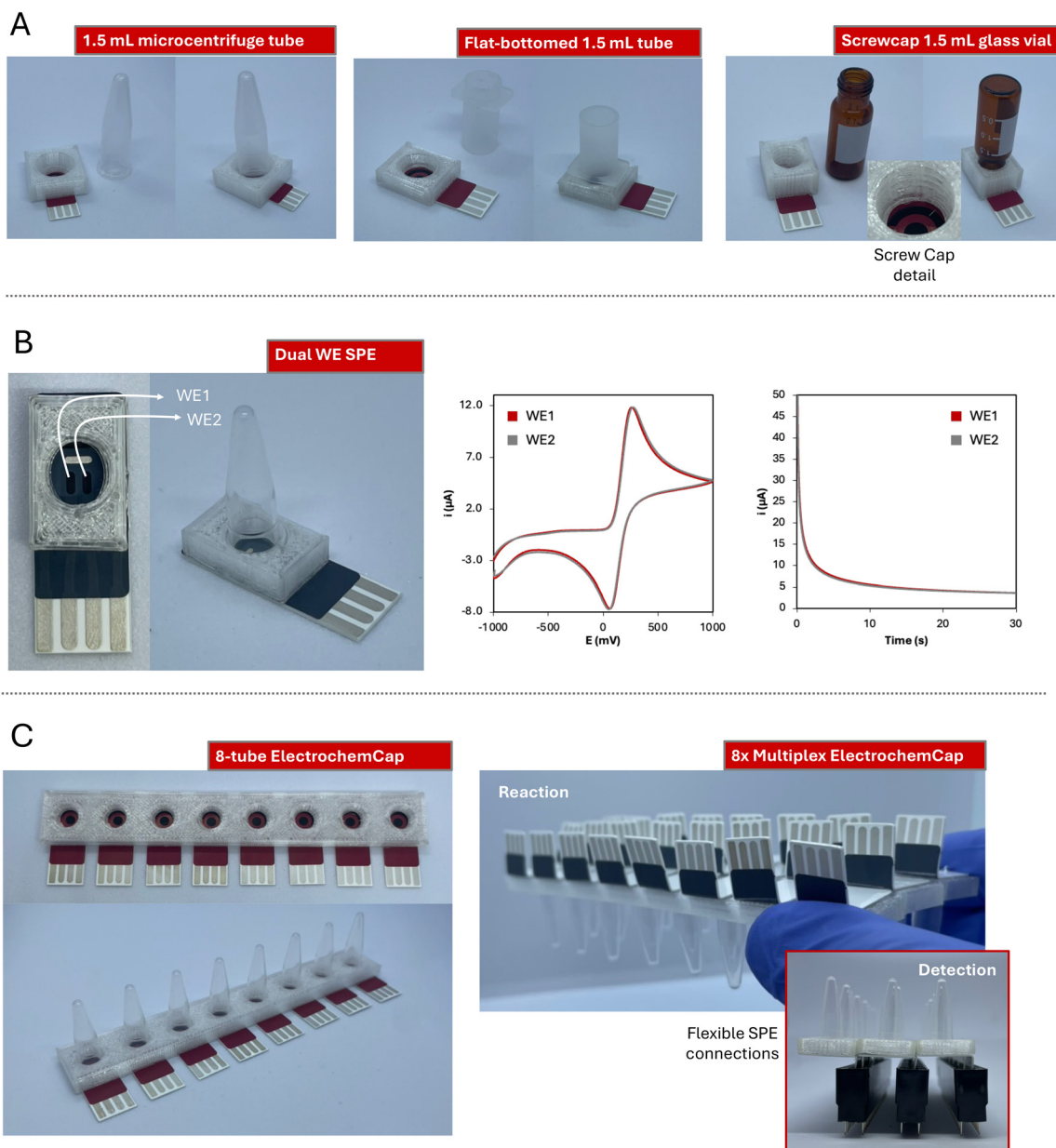


**Fig. 3** Additional ElectrochemCap designs. A) Pictures of the models adapted to different 1.5 mL tubes. Left: Microcentrifuge tube; centre: flat-bottomed; right: screwcap glass vial. A detail of the screwcap TPU piece is shown. B) Dual WE SPE model. Left: Picture of the model. Centre: CV curves recorded with both WEs in 100  $\mu\text{L}$  of 5 mM  $\text{K}_4[\text{Fe}(\text{CN})_6]$  in PBS at a scan rate of  $0.1 \text{ V s}^{-1}$ . Right: Chronoamperograms recorded in both WEs applying  $+0.6 \text{ V}$  for 30 s. C) Multiplexed designs. Left: 8-Tube ElectrochemCap model; right: 8 $\times$  triple ElectrochemCap model. A lateral view of the device is shown, as well as a three 8 $\times$  row device connected to three pin header connectors.



peak potential,<sup>34</sup> which was evaluated for different initial concentrations of SARS-CoV-2 RNA.

The results of the calibration curve using electrochemical readout are shown in Fig. 2C. Pictures of the tubes coupled to the ElectrochemCap after the RT-LAMP reaction are presented at the top. This method presents a linear range between 20 and 1500 copies per  $\mu\text{L}$ ,<sup>30</sup> with a determination equation defined as  $\Delta E_p$  (mV) = 21 log[RNA] (copies per  $\mu\text{L}$ ) – 18, with a determination coefficient of  $R^2 = 0.993$ . Furthermore, as the reaction is performed at 65 °C, the device was also evaluated in terms of water loss. For this purpose, LAMP reaction solutions were weighed before and after the reaction, resulting in a weight loss lower than 2.5% ( $n = 10$ ).

We established a negative cutoff level for  $\Delta E_p$  of 5 mV (3 times the standard deviation of the blank, *i.e.*, negative control). Thus, a sample with a potential shift beyond this value would be considered as positive. On the other hand, a value of 52 mV is also considered a limit, based on the  $\Delta E_p$  of the highest measured copy number plus 3 times its standard deviation. Beyond this value, samples could be considered positive but out of the linear range, with a copy number over 1500 copies per  $\mu\text{L}$ . This method presents a theoretical LOD of 2 copies per  $\mu\text{L}$  (obtained as 3 times the standard deviation of the blank divided by the slope of the calibration curve). However, we consider a practical LOD of 20 copies per  $\mu\text{L}$ , as amplifications with a lower copy number (*e.g.*, 10 copies per  $\mu\text{L}$ , the grey dataset in Fig. 3C) showed the limit of the error bar for  $\Delta E_p$  below the cutoff. This method presents an LOD very similar to the previous reported method.<sup>30</sup> Although some RT-qPCR procedures show a LOD lower than the obtained with this method (0.1 *vs.* 2 copies per  $\mu\text{L}$ ),<sup>35</sup> both are appropriate, providing LAMP methodology a faster, non-centralized alternative.

To validate this method, 4 nasopharyngeal (NP) swab samples were collected and analyzed following this methodology. The samples were initially analyzed undiluted, where the RT-qPCR negative samples showed a  $\Delta E_p$  under the cutoff, and RT-qPCR positive samples presented a  $\Delta E_p$  beyond the linear range (Fig. 2D). To prove the linearity of the method and quantify the positive samples, serial dilutions of said samples were performed (1:5, 1:50 and 1:100) and then analyzed *via* RT-LAMP-ED with the ElectrochemCap (Fig. 2D, orange dataset). The results showed concentrations of  $2.9 \times 10^3$  and  $4.6 \times 10^3$  copies per  $\mu\text{L}$  for samples 3 and 4, correlating with their PCR Ct (threshold cycle) values of 28 and 18, respectively. Representations for the different dilutions of samples 3 and 4 showed determination coefficients of 0.992 and 0.9991, respectively, with slopes very close to that of the calibration curve, inferring that matrix effects were negligible (Fig. S3†).

### Adaptations of the ElectrochemCap

Even though this work has focused on the application of the ElectrochemCap to LAMP reaction detection, this device is not limited only to this use. The ElectrochemCap is a versatile

platform for any (bio)electroanalytical purpose that could be carried out in a microcentrifuge tube. Although the model proposed here is limited to 200  $\mu\text{L}$  PCR tubes, this innovative device could pave the way to multiple applications by introducing variations, not only in terms of volume, but also material, shape, *etc.* Then, issues such as material compatibility, reaction stirring or continuous monitoring, as well as the possibility of performing multiplexed analysis could be considered. For this purpose, several other models have been designed to widen the possibilities of the ElectrochemCap.

The first adaptation of the design has considered the possibility of using different volumes of the reaction solution and thus, of the tubes used. The 1.5 mL microcentrifuge tube is among the most used consumable materials in many laboratories. Thus, a model adapted to it has been developed (pictures in Fig. 3A left, adapted design in Fig. S4A†). This provides a platform over 200  $\mu\text{L}$  for reactions such as enzymatic assays or immunoassays, among others, usually performed in larger volumes. Furthermore, it could be also extrapolated to other liquid containers, such as flat-bottomed tubes (Fig. 3A center, adapted design in Fig. S4B†) or screwcap glass vials (Fig. 3A right, adapted design in Fig. S4C†). This provides a platform for i) tubes based on different materials (*e.g.*, polymers or glass) and ii) assays in curve or flat-bottomed tubes, enabling the last ones magnetic stirring with small bars included. In the case of the glass vial, the snap cap has been modified into a screwcap, opening the door for adaptations to any other screwcap container.

Regarding the electrochemical cell, this device can integrate SPE cards containing not only different electrode materials (gold, platinum, modified carbon...) but also cell designs. Including two working electrodes is very advantageous for different (bio)applications, such as the simultaneous detection of different analytes by performing different modifications on each working electrode,<sup>36,37</sup> increasing the precision of the measurements or reducing the interference from noise/drift or other electroactive elements.<sup>38</sup> In this case, we have also incorporated a dual-working electrode (WE1 and WE2 in Fig. 3B, adapted design in Fig. S4C†) screen-printed electrochemical cell. This device has been evaluated using 100  $\mu\text{L}$  of 5 mM  $\text{K}_4[\text{Fe}(\text{CN})_6]$ , both using cyclic voltammetry and chronoamperometry (Fig. 3B). This last technique results very convenient for decentralized analysis, since, instead of performing a potential scan, a single potential is applied and an *i-t* curve is recorded. This cell has shown a great electrochemical performance regarding both current intensity and potential measured for the two WEs ( $E_{pa}$  of 260 and 269 mV;  $I_{pa}$  of 106.5 and 106.0  $\mu\text{A}$  by cyclic voltammetry; current intensity by chronoamperometry of 3.76 and 3.86  $\mu\text{A}$  at 30 s).

In the field of multiplexed analysis, an 8-tube platform cap has also been designed (Fig. 3C, adapted design in Fig. S4D†). It could be coupled to an 8-channel potentiostat or to 8 USB-based potentiostats, providing 8 simultaneous measurements in just one flip. Cards with 8-channel SPE-cells have been widely used for bioanalytical applications, where, with just one platform, several samples could be analyzed for one analyte determination.





Alternatively, several replicates of one sample can be measured to evaluate the precision. Furthermore, several analytes could be also analyzed in just one reaction, or calibration curves can be obtained in just one batch. This has been applied in several fields such as exosome profiling,<sup>39</sup> detection of DNA point-mutations<sup>40</sup> or quantum-dot determination,<sup>41</sup> amongst others. Furthermore, this design could be expanded, generating a device containing any tube quantity multiple of 8. To have fully functional platforms, and thanks to the flexibility of the substrate material (350  $\mu\text{m}$  thick PET), the SPE connections can be bent (Fig. 3C right top). Thus, electrochemical cells can be adhered to the 8-tube caps and the connections from interior cards can be accessed. With that, the 8-tube rows (3 in this case) could be easily connected to the potentiostat through common pin connectors for multiplexing options (Fig. 3C right bottom).

## Conclusions

In this work, we have developed the ElectrochemCap, a simple and marketable electrochemical platform based on a microcentrifuge tube cap. The device is an affordable innovation that can be used for any electroanalytical approach combining a microcentrifuge tube, a SPE and materials as simple as TPU and adhesive layers. This device presents a robust and precise behaviour in a wide range of microvolumes, with RSDs of the analytical signal under 4% for volumes spanning from 50 to 200  $\mu\text{L}$ .

Furthermore, we have applied it to the electrochemical detection of SARS-CoV-2 by RT-LAMP reactions. A previous method described by the group, where off-line detection was employed, was successfully adapted to the use of the ElectrochemCap. Integration of the electrochemical detection allows on-line operation, showing, as in the previous case, good analytical parameters such as linear range, sensitivity or LOD, but avoiding the manipulation of the amplification and consequently, carryover contamination. Furthermore, the LAMP-ElectrochemCap has been validated with clinical samples, showing 100% coincidence with RT-qPCR results, and concurring with Ct results.

We have additionally designed several devices, increasing the possibilities of the interface (regarding volume, material or multiplexed analysis). Additionally, this design also allows any modification of the SPE card or the containers, with *e.g.*, nanomaterials or recognition elements, to create new integrated platforms for bioanalysis. We are currently working on adapting this device to other bioassays and generalizing its use into the bioelectroanalytical practice, as well as combining it with fully portable equipment (smartphone-powered heaters and potentiostats) to obtain field-deployable integrated laboratory procedures.

## Data availability statement

The data that support the findings of this study, including the ESI,† are available at the Repository of the University of Oviedo (RUO) at the URL: <https://digibuo.uniovi.es/dspace/>

[handle/10651/73040](https://doi.org/10.1039/C4LC00000A), with the following DOI: [https://doi.org/10.17811/ruo\\_datasets.73040](https://doi.org/10.17811/ruo_datasets.73040).

## Author contributions

Pablo Rioboó-Legaspi: conceptualization, investigation, formal analysis, data curation, visualization, and writing – original draft. Estefanía Costa-Rama: conceptualization, methodology, supervision, visualization, writing – review & editing, funding acquisition, and project administration. M. Teresa Fernández-Abedul: conceptualization, methodology, supervision, visualization, writing – review & editing, and funding acquisition.

## Conflicts of interest

M. T. F.-A. declares that she was one of the founders of MicruX Technologies, a company engaged in the development of miniaturized electrodes and electrochemical/microfluidic equipment and remains a consultant and shareholder. She declares that it has not influenced the work reported in this paper. The rest of the authors declare no competing financial interest.

## Acknowledgements

This work was supported by the I+D+i projects PID2020-118376RA-I00 (funded by MCIN/AEI/10.13039/501100011033) and AYUD/2021/51289 (from the PCTI Program of the Government of the Principality of Asturias and the FEDER Program of the EU). P. R. L. was supported by the Asturian Council for Science, Technology, and Innovation “Severo Ochoa” grant (BP21-029) and E. C. R. by the Spanish Ministry of Universities “Beatriz Galindo” grant (BG20-00027). The authors would like to acknowledge the technical support provided by Servicios Científico-Técnicos of the University of Oviedo and by the Service of Microbiology and Emergency Care of the Hospital Universitario Central de Asturias.

## References

- 1 T. Notomi, H. Okayama, H. Masubuchi, T. Yonekawa, K. Watanabe and N. Amino, *et al.*, Loop-mediated isothermal amplification of DNA, *Nucleic Acids Res.*, 2000, **28**, e63.
- 2 B. B. Oliveira, B. Veigas and P. V. Baptista, Isothermal amplification of nucleic acids: the race for the next “Gold Standard”, *Front. Sens.*, 2021, **2**, 752600.
- 3 S. Sen, P. Bhowmik, S. Tiwari, Y. Peleg and B. Bandyopadhyay, Versatility of reverse transcriptase loop-mediated isothermal amplification (RT-LAMP) from diagnosis of early pathological infection to mutation detection in organisms, *Mol. Biol. Rep.*, 2024, **51**, 211.
- 4 S. Leonardo, A. Toldrà and M. Campàs, Biosensors based on isothermal DNA amplification for bacterial detection in food safety and environmental monitoring, *Sensors*, 2021, **21**, 1.
- 5 J. Lei, X. Han, X. Tang, H. Wang and Q. Zhang, Development of anti-idiotypic nanobody-phage based Immuno-Loop-



- Mediated Isothermal Amplification assay for aflatoxins in peanuts, *Toxins*, 2020, **12**, 565.
- 6 S. Ayaz Kök, S. Üstün and S. H. Taşkent, Diagnosis of ruminant viral diseases with Loop-Mediated Isothermal Amplification, *Mol. Biotechnol.*, 2023, **65**, 1228.
  - 7 S. Kubo, H. Niimi and I. Kitajima, Duplex loop-mediated isothermal amplification assay for simultaneous detection of human and human male DNA, *BMC Res. Notes*, 2023, **16**, 180.
  - 8 A. Knox, G. Zerna and T. Beddoe, Current and future advances in the detection and surveillance of biosecurity-relevant equine bacterial diseases using Loop-Mediated Isothermal Amplification (LAMP), *Animals*, 2023, **13**, 2663.
  - 9 J. Akter, W. J. M. Smith, M. Gebrewold, I. Kim, S. L. Simpson and A. Bivins, *et al.*, Evaluation of colorimetric RT-LAMP for screening of SARS-CoV-2 in untreated wastewater, *Sci. Total Environ.*, 2024, **907**, 167964.
  - 10 J. T. Connelly, J. P. Rolland and G. M. Whitesides, "Paper Machine" for molecular diagnostics, *Anal. Chem.*, 2015, **87**, 7595.
  - 11 J. M. Marangoni, K. K. S. Ng and A. Emadi, Strategies for the voltammetric detection of Loop-Mediated Isothermal Amplification, *Micromachines*, 2023, **14**, 472.
  - 12 P. S. Ganesh and S. Y. Kim, A comparison of conventional and advanced electroanalytical methods to detect SARS-CoV-2 virus: A concise review, *Chemosphere*, 2022, **307**, 135645.
  - 13 S.-H. Kim, S.-Y. Lee, U. Kim and S.-W. Oh, Diverse methods of reducing and confirming false-positive results of loop-mediated isothermal amplification assays: A review, *Anal. Chim. Acta*, 2023, **1280**, 341693.
  - 14 J. Kampeera, P. Pasakon, C. Karuwan, N. Arunrut, A. Sappat and S. Sirithammajak, *et al.*, Point-of-care rapid detection of *Vibrio parahaemolyticus* in seafood using loop-mediated isothermal amplification and graphene-based screen-printed electrochemical sensor, *Biosens. Bioelectron.*, 2019, **132**, 271.
  - 15 A. Rodríguez-Penedo, P. Rioboó-Legaspi, A. González-López, A. Lores-Padín, R. Pereiro and M. d. M. García-Suárez, *et al.*, Electrocatalytic Palladium Nanoclusters as versatile indicators of bioassays: Rapid electroanalytical detection of SARS-CoV-2 by Reverse Transcription Loop-Mediated Isothermal Amplification, *Adv. Healthcare Mater.*, 2023, **12**, 2202972.
  - 16 A. Saxena, P. Rai, S. Mehrotra, S. Baby, S. Singh and V. Srivastava, *et al.*, Development and clinical validation of RT-LAMP-based Lateral-Flow devices and electrochemical sensor for detecting multigene targets in SARS-CoV-2, *Int. J. Mol. Sci.*, 2022, **23**, 13105.
  - 17 P. Rioboó-Legaspi, N. Rabanal-Rubio, E. Costa-Rama, M. D. Cima-Cabal, M. d. M. García-Suárez and M. T. Fernández-Abedul, Malachite green as a dual visual/electrochemical indicator for loop-mediated isothermal amplification: Application to SARS-CoV-2 detection, *Microchem. J.*, 2024, **198**, 110172.
  - 18 A. Rivas-Macho, U. Eletxigerra, R. Diez-Ahedo, Á. Barros, S. Merino and F. Goñi-de-Cerio, *et al.*, Development of an electrochemical sensor for SARS-CoV-2 detection based on Loop-Mediated Isothermal Amplification, *Biosensors*, 2023, **13**, 924.
  - 19 A. Rivas-Macho, U. Eletxigerra, R. Diez-Ahedo, S. Merino, A. Sanjuan and M. M. Bou-Ali, *et al.*, Design and 3D printing of an electrochemical sensor for *Listeria monocytogenes* detection based on loop mediated isothermal amplification, *Heliyon*, 2023, **9**, e12637.
  - 20 A. Martin, K. B. Grant, F. Stressmann, J. M. Ghigo, D. Marchal and B. Limoges, Ultimate single-copy DNA detection using real-time electrochemical LAMP, *ACS Sens.*, 2016, **1**, 904.
  - 21 N. Y. Jayanath, L. T. Nguyen, T. T. Vu and L. D. Tran, Development of a portable electrochemical loop mediated isothermal amplification (LAMP) device for detection of hepatitis B virus, *RSC Adv.*, 2018, **8**, 34954.
  - 22 A. Ainla, M. P. S. Mousavi, M.-N. Tsaloglou, J. Redston, J. G. Bell and M. T. Fernandez-Abedul, *et al.*, Open-source potentiostat for wireless electrochemical detection with smartphones, *Anal. Chem.*, 2018, **90**, 6240.
  - 23 D. Martín-Yerga, I. Álvarez-Martos, M. C. Blanco-López, C. S. Henry and M. T. Fernández-Abedul, Point-of-need simultaneous electrochemical detection of lead and cadmium using low-cost stencil-printed transparency electrodes, *Anal. Chim. Acta*, 2017, **981**, 24.
  - 24 A. C. Glavan, A. Ainla, M. M. Hamedi, M. T. Fernández-Abedul and G. M. Whitesides, Electroanalytical devices with pins and thread, *Lab Chip*, 2016, **16**, 112.
  - 25 A. González-López, E. Costa-Rama, C. G.-C. Fernández, L. Benavente-Fernández, S. Calleja-Puerta, B. Fernández-García, R. Pereiro and M. T. Fernández-Abedul, Microcentrifuge Tubes as Disposable Immunoelectrochemical Cells for the On-Site Determination of GFAP, Biomarker of Hemorrhagic Stroke, *Proceedings*, 2020, **60**(1), 10.
  - 26 M. U. Ahmed, M. Saito, M. M. Hossain, S. R. Rao, S. Furui and A. Hino, *et al.*, Electrochemical genosensor for the rapid detection of GMO using loop-mediated isothermal amplification, *Analyst*, 2009, **134**, 966.
  - 27 Z. Xu, K. Yin, X. Ding, Z. Li, X. Sun and B. Li, *et al.*, An integrated E-Tube Cap for sample preparation, Isothermal Amplification and label-free electrochemical detection of DNA, *Biosens. Bioelectron.*, 2021, **186**, 113306.
  - 28 J. F. Hernández-Rodríguez, F. Della Pelle, D. Rojas, D. Compagnone and A. Escarpa, Xurography-enabled thermally transferred carbon nanomaterial-based electrochemical sensors on polyethylene terephthalate-ethylene vinyl acetate films, *Anal. Chem.*, 2020, **92**, 13565.
  - 29 R. M. Cardoso, C. Kalinke, R. G. Rocha, P. L. dos Santos, D. P. Rocha and P. R. Oliveira, *et al.*, Additive-manufactured (3D-printed) electrochemical sensors: A critical review, *Anal. Chim. Acta*, 2020, **1118**, 73.
  - 30 P. Rioboó-Legaspi, A. González-López, J. F. Beltrán-Sánchez, M. D. Cima-Cabal, M. M. García-Suárez and A. J. G. Sánchez, *et al.*, Phenol red as electrochemical indicator for highly sensitive quantification of SARS-CoV-2 by loop-mediated isothermal amplification detection, *Talanta*, 2023, **266**, 124963.
  - 31 J. Saez, L. Basabe-Desmonts and F. Benito-Lopez, Low-cost origami fabrication of 3D self-aligned hybrid microfluidic structures, *Microfluid. Nanofluid.*, 2016, **20**, 1781.



- 32 C. Batéjat, Q. Grassin, J.-C. Manuguerra and I. Leclercq, Heat inactivation of the severe acute respiratory syndrome coronavirus 2, *J. Biosaf. Biosecur.*, 2021, **3**, 1.
- 33 A. Boubakri, N. Guermazi, K. Elleuch and H. F. Ayedi, Study of UV-aging of thermoplastic polyurethane material, *Mater. Sci. Eng., A*, 2010, **527**, 1649.
- 34 A. González-López, M. D. Cima-Cabal, P. Rioboó-Legaspi, E. Costa-Rama, M. M. García-Suárez and M. T. Fernández-Abedul, Electrochemical detection for isothermal loop-mediated amplification of pneumolysin gene of *Streptococcus pneumoniae* based on the oxidation of phenol red indicator, *Anal. Chem.*, 2022, **94**, 13061.
- 35 R. Arnaout, R. A. Lee, G. R. Lee, C. Callahan, C. F. Yen and K. P. Smith, *et al.*, SARS-CoV2 testing: The limit of detection matters, *bioRxiv*, 2020, preprint, DOI: [10.1101/2020.06.02.131144](https://doi.org/10.1101/2020.06.02.131144).
- 36 A. Soleh, P. Kanatharana, P. Thavarungkul and W. Limbut, Novel electrochemical sensor using a dual-working electrode system for the simultaneous determination of glucose, uric acid and dopamine, *Microchem. J.*, 2020, **153**, 104379.
- 37 R. A. Sánchez-Moreno, M. Gismera, A. J. Sevilla and M. A. T. Procopio JR, Potentiometric screen-printed bisensor for simultaneous determination of chromium(III) and chromium(VI), *Electroanalysis*, 2011, **23**, 287.
- 38 M. Lv, X. Qiao, Y. Li, X. Zeng and X. Luo, A stretchable wearable sensor with dual working electrodes for reliable detection of uric acid in sweat, *Anal. Chim. Acta*, 2024, **1287**, 342154.
- 39 S. Jeong, J. Park, D. Pathania, C. M. Castro, R. Weissleder and H. Lee, Integrated magneto-electrochemical sensor for exosome analysis, *ACS Nano*, 2016, **10**, 1802.
- 40 R. Sebuyoya, A. Valverde, L. Moranova, J. Strmiskova, R. Hrstka and V. R.-V. Montiel, *et al.*, Dual detection system for cancer-associated point mutations assisted by a multiplexed LNA-based amperometric bioplatfrom coupled with rolling circle amplification, *Sens. Actuators, B*, 2023, **394**, 134375.
- 41 D. Martín-Yerga and A. Costa-García, Electrochemical detection of quantum dots by stabilization of electrogenerated copper species, *Electrochem. Commun.*, 2017, **74**, 53.

